50. TRACE ELEMENT CONTENTS OF CARBONATES FROM HOLES 549 AND 550B (LEG 80): COMPARISON WITH SOME TETHYAN AND ATLANTIC SITES[1]

Annick Andrianiazy and Maurice Renard, Département de Géologie Sédimentaire, Université Pierre et Marie Curie[2]

ABSTRACT

The evolution through time of trace element contents (Sr, Mg, Mn, and Fe) of sediments at Sites 549 and 550 is similar to that of previously studied oceanic sites. A comparison with some North Atlantic sites and with outcrops of the Gubbio section (Italy) allowed us to show that

1. A negative correlation between Sr and Mg contents, generally characteristic of pelagic carbonate having undergone diagenesis, is confirmed.
2. Magnesium diagenesis occurs over a relatively short time and is sensitive to the sedimentation rate of each individual time period, whereas Sr diagenesis is a long-term phenomenon and is sensitive to the overall average sedimentation rate at the site. Strontium loss by sediments is related to sediment age (i.e., residence time of sediments in a given diagenetic environment) and could be a rough method of dating individual sediment layers.
3. The nature of the seafloor (oceanic or continental) does not appear to play an important part in the content of Fe and Mn in sediments. Their distribution depends more on mid-oceanic ridge activity, paleodepth (through mediation of $CaCO_3$ dissolution and environment), and distance of the site from the ridge.

INTRODUCTION

Previous studies of sediments from Holes 390, 391, 392, 398C, 400A, 516F, and 116 (Renard et al., 1978, 1979, 1982) have shown the potential use of Sr as a time marker for pelagic carbonate diagenesis (because of Sr loss with time). Also, the manganese–iron couple appears to be an indicator of submarine volcano-hydrothermal activity. Moreover, the study of pelagic facies from continental outcrops, such as from the Gubbio section of Umbria, Italy, has shown a negative Sr/Mg correlation characteristic of the diagenesis of pelagic carbonates, whereas this correlation is positive for diagenesis of continental shelf carbonates. Because of the high Mg concentration of interstitial waters, the relationship between Sr and Mg in sediments has rarely been studied at DSDP sites.

The aim of the present work is therefore (1) to test the generality of the negative Sr/Mg relationship in oceanic carbonates (for this purpose, the sediments were washed to eliminate Mg from their interstitial waters), and (2) to compare the geochemistry of Fe and Mn in carbonates on continental crust (Site 549) with those on oceanic crust (Site 550).

METHODS

The geochemistry of trace elements was studied on 141 samples from Hole 549 ranging in age from Pleistocene to Barremian and on 45 samples from Hole 550B ranging in age from early Paleocene to late Albian.

After being crushed, the samples were washed to eliminate interstitial water. The washes consisted of multiple (an average of 12) centrifugations with distilled water. The conductivity of the wash water was measured after each centrifugation, and the treatment was stopped when the conductivity of the wash water stopped decreasing and reached a plateau. X-ray diffraction of the carbonate samples showed mainly the presence of low-Mg calcite. Some samples containing dolomite were eliminated from the study. After this pretreatment, samples were dissolved in 1 *N* acetic acid. Trace element analysis was conducted by atomic absorption spectrometry using the methods described by Renard and Blanc (1971, 1972). The data are summarized in Table 1.

RESULTS

Strontium

Sr contents in carbonates from Hole 549 range from 1400–1500 ppm for Miocene–Oligocene aged sediments to 400 ppm for Cenomanian sediments (Fig. 1). This decrease with age is caused by increasing diagenesis with depth. It should be noted that the loss of Sr is not regular. Sediments deposited during certain periods, such as Eocene and mid-Cretaceous, are impoverished in Sr, whereas others deposited during Albian, late Paleocene, and late Oligocene time are enriched in comparison to the average curve. These divergences could have a stratigraphic significance (Renard et al., 1982). Similarly for Hole 550B, a decrease with age in Sr can be observed: from 1200 ppm in lower Paleocene sediments to 500 ppm in Santonian–Coniacian sediments (Fig. 1). Sr-rich (Albian–Cenomanian) and Sr-poor periods (middle–Late Cretaceous) also exist in this hole.

The variations of average Sr concentrations in interstitial waters at Site 549 (Gieskes, this volume) are plotted in Figure 2. For at least up through Eocene time, this plot is the inverse of the plot of Sr concentration in sediments (Fig. 2), thus helping to confirm the influence of recrystallization in Sr distribution.

That the variation in Sr concentrations in interstitial waters is related to sedimentation rate has been clearly shown by Manheim et al. (1971; Leg 8) and by Gieskes

---

[1] Graciansky, P. C. de, Poag, C. W., et al., *Init. Repts. DSDP*, 80: Washington (U.S. Govt. Printing Office).

[2] Addresses: (Andrianiazy) Département de Géologie Sédimentaire, Université Pierre et Marie Curie (Paris VI) et Bureau Recherche Géologique et Minière Orléans; (Renard) Département de Géologie Sédimentaire, Université Pierre et Marie Curie (Paris VI) et Laboratoire Associé au Centre National de la Recherche Scientifique 319.

Table 1. Summary of results—Holes 549, 549A, 550B.

Core-Section (interval in cm)	$CaCO_3$ (%)	Mg (ppm)	Sr (ppm)	Mn (ppm)	Fe (ppm)
Hole 549					
1-5, 58–60	75.94	1666	1140	775	130
2-1, 38–40	79.71	1492	1220	829	263
3-1, 4–6	79.47	1554	1111	798	183
4-1, 105–107	65.31	1447	1457	716	170
4-5, 105–107	74.56	1648	1160	1055	240
5-1, 54–55	77.83	1632	1126	1061	335
5-3, 54–55	73.16	1658	1121	1102	270
6-1, 68–69	71.53	1669	1168	1052	112
6-5, 68–69	65.55	1920	1186	1027	60
7-1, 37–39	66.02	1877	1181	1085	84
7-5, 67–69	68.84	1774	1113	936	124
8-1, 79–80	74.27	1741	1020	939	100
8-3, 79–80	76.28	1609	1065	885	94
9-1, 44–45	74.88	1617	1060	1124	142
9-3, 29–30	74.40	1575	1046	1163	124
10-1, 77–78	76.28	1690	1073	898	20
10-3, 81–83	58.84	1346	1090	1188	17
10-5, 60–62	78.51	1475	1069	902	15
11-1, 106–108	66.92	1913	1275	3827	28
11-5, 115–117	46.84	2280	1295	3160	65
12-1, 60–62	52.19	1761	1206	3177	55
12-3, 54–56	45.59	2437	1210	3046	62
13-1, 63–65	71.81	1430	953	2780	70
13-5, 64–66	79.80	1457	806	1953	78
14-1, 64–66	78.33	1447	831	1220	76
14-5, 22–24	69.25	1808	996	2924	199
15-1, 61–62	50.56	2095	1017	2352	221
15-3, 60–62	38.97	3184	1180	2077	152
15-5, 61–63	49.57	2800	1074	2262	225
16-1, 62–63	51.34	2739	1054	2702	316
16-3, 58–59	57.23	2179	963	2996	391
16-5, 64–65	42.89	4300	996	1766	110
17-1, 69–70	63.35	1580	1051	1880	8
17-5, 71–72	52.19	1779	1089	1810	8
18-1, 68–69	61.12	1961	1198	1684	11
18-3, 46–47	45.76	2297	1140	1716	11
19-1, 19–20	47.78	2845	1057	2269	8
19-3, 34–35	74.92	1662	972	2302	12
20-1, 24–25	63.80	1644	1164	2376	26
20-3, 20–21	68.48	1496	1145	2914	54
20-5, 13–14	75.27	1182	1074	2372	50
21-2, 2–3	76.54	1090	1107	1849	41
22-2, 109–110	93.48	1056	819	439	15
22-4, 93–94	93.92	1045	800	677	18
23-2, 65–67	92.31	934	800	390	11
23-4, 54–56	94.89	886	746	282	12
24-2, 28–30	91.43	928	678	911	17
25-2, 37–39	81.91	1185	615	654	25
26-1, 7–9	88.98	1456	455	922	145
27-1, 0–3	52.02	1018	692	987	525
28-2, 28–30	75.32	2157	472	570	247
29-1, 34–37	73.35	2311	373	635	239
32-1, 27–29	22.51	7940	714	1666	1652
34-1, 53–54	41.67	5606	404	1143	4268
34-1, 70–73	29.31	5879	680	1168	2436
35-1, 44–46	28.59	7735	753	1692	1867
36-1, 17–18	40.58	6590	397	778	4487
37-1, 21–22	25.34	6664	954	1087	1261
37-2, 34–36	32.80	6522	753	1879	1944
40-1, 17–20	28.42	5265	705	723	93
42-1, 64–66	32.63	4981	676	1682	2148
42-3, 85–86	34.01	6941	829	1876	1531
43-2, 90–93	32.74	7647	835	2095	1200
43-4, 53–54	29.86	7065	775	1981	1252
44-2, 2–4	33.12	6781	603	1372	1616
44-4, 2–4	31.00	6481	594	1593	2295
45-2, 61–63	29.45	6956	673	1797	1693

Table 1. (Continued).

Core-Section (interval in cm)	$CaCO_3$ (%)	Mg (ppm)	Sr (ppm)	Mn (ppm)	Fe (ppm)
Hole 549 (Cont.)					
45-4, 34–35	30.00	6730	604	1743	1390
46-2, 96–99	28.37	6260	698	1762	1642
46-4, 93–94	40.89	4969	657	1834	2804
47-2, 90–91	39.32	5313	612	753	1297
47-4, 20–21	44.65	4877	617	1238	2129
54-4, 0–2	42.26	9248	451	591	5052
55-4, 124–126	63.73	3948	321	521	4369
56-2, 53–55	49.60	7085	483	561	6384
56-4, 43–46	29.46	11012	550	565	6718
57-2, 62–64	19.34	18293	637	599	10199
57-4, 121–123	35.73	7552	430	503	10824
58-2, 56–57	23.48	9890	545	580	8779
58-6, 79–80	43.28	7325	508	611	7503
59-2, 40–42	27.94	12223	588	722	7916
60-2, 27–29	42.68	7663	453	675	9625
60-6, 70–72	29.91	7156	532	100	7156
61-2, 56–58	11.99	12340	965	559	4486
61-4, 116–118	17.72	7660	740	799	5453
74-2, 21–23	14.22	11419	589	1035	13516
75-2, 57–59	67.20	5600	550	597	8670
79-1, 32–34	39.50	6061	288	1212	8323
80-1, 51–53	49.23	4577	552	2284	6567
99-1, 145–146	58.94	11865	297	9875	15193
Hole 549A					
4-3, 105–109	82.38	1429	1394	183	38
5-2, 32–36	84.43	1190	1445	238	29
6-2, 44–48	80.30	1339	1542	370	20
7-3, 73–78	88.74	1150	1353	579	6
8-3, 16–20	87.91	1135	1311	462	13
9-2, 114–118	87.36	1116	1438	590	38
10-4, 74–78	85.88	968	1543	549	37
11-3, 74–78	83.25	1477	1298	727	5
12-1, 96–100	85.41	1329	1351	717	10
13-1, 90–94	84.91	1164	1412	666	49
13-3, 116–120	87.39	1043	1398	706	192
14-1, 86–90	83.40	970	1520	622	175
15-1, 60–64	83.18	1207	1450	628	190
15-2, 64–68	86.22	1008	1471	798	186
16-1, 76–80	87.22	995	1464	661	162
17-1, 53–57	85.84	1195	1453	821	143
17-2, 14–18	86.85	1041	1513	633	138
18-1, 76–80	91.62	1016	1291	600	156
19-1, 28–32	90.57	973	1286	615	184
20-1, 48–52	89.38	967	1289	557	234
21-1, 34–38	91.83	1022	1209	676	182
24-1, 57–60	84.04	1253	1361	653	34
24-2, 66–70	91.72	1119	1244	795	42
25-2, 82–86	89.33	1070	1301	726	45
26-1, 48–52	85.67	1093	1335	580	20
27-1, 93–97	86.56	1209	1269	877	24
28-1, 111–115	86.54	1200	1263	749	28
32-2, 22–25	84.25	1374	1210	1019	20
33-2, 46–50	85.17	1136	1339	950	19
34-1, 62–65	84.43	1048	1387	790	23
35-1, 16–19	81.29	1397	1300	750	21
36-1, 10–15	85.12	1150	1314	849	36
37-1, 4–9	85.12	1074	1356	795	56
38-1, 36–39	80.77	1145	1254	853	198
39-2, 22–25	79.47	1338	1254	819	83
40-1, 53–56	77.85	1229	1375	841	156
41-1, 13–16	80.21	1468	1267	706	150
42-1, 30–33	82.39	1365	1244	1030	150
Hole 550B					
1-3, 9–14	61.57	791	1099	1417	304

Table 1. (Continued).

Core-Section (interval in cm)	$CaCO_3$ (%)	Mg (ppm)	Sr (ppm)	Mn (ppm)	Fe (ppm)
Hole 550B (Cont.)					
1-3, 63-66	62.76	948	1120	2252	682
2-2, 33-36	58.57	1283	762	1585	13
2-2, 37-40	89.32	1487	848	1143	17
3-1, 109-114	82.74	706	917	840	7
4-1, 57-60	75.87	658	1035	1262	12
5-2, 70-73	85.73	619	856	1424	23
5-2, 127-131	89.13	708	819	1102	33
5-4, 28-31	85.82	663	982	1514	45
5-4, 140-143	93.37	876	853	1425	46
7-1, 60-63	49.03	1139	1205	722	39
8-1, 41-44	92.92	1553	695	1473	217
8-1, 114-117	92.90	2090	514	1640	393
8-3, 76-79	89.71	982	812	1120	230
9-1, 110-113	80.55	1092	862	3392	871
9-4, 52-56	58.75	811	1229	1651	519
9-4, 96-99	91.00	654	954	2123	598
10-1, 61-64	51.76	1088	1152	1420	476
10-3, 114-117	62.15	776	1210	1670	477
10-5, 40-44	51.23	1044	1311	1608	359
11-1, 96-100	87.08	877	881	1355	304
11-3, 80-83	37.95	2388	1271	1741	229
12-2, 42-45	92.45	1553	687	2055	268
12-4, 90-93	75.84	843	839	1726	59
13-1, 40-43	94.12	1162	634	2483	134
13-1, 89-93	91.30	1229	449	2616	380
13-2, 76-79	73.99	862	704	1896	38
15-5, 73-79	80.26	862	753	3293	654
16-2, 87-91	74.63	927	747	4522	973
17-1, 120-124	73.83	865	790	3972	1032
17-2, 125-128	72.33	887	850	3316	891
17-5, 63-70	75.39	831	760	3760	927
18-7, 66-69	73.53	973	804	3151	767
20-2, 113-118	57.78	1371	914	2362	449
20-4, 17-20	74.00	1520	596	2534	788
21-2, 41-44	48.93	1548	952	1040	487
21-5, 25-28	64.04	1133	858	2010	1513
22-1, 74-77	58.98	1459	899	2225	1809
22-3, 119-122	59.63	1286	838	1624	1529
22-5, 54-57	68.33	1566	746	2722	2051
23-1, 18-21	61.87	1378	779	2122	1780
23-3, 96-99	64.50	1306	683	2388	1918
24-2, 60-63	51.14	1558	798	1854	1239
25-1, 47-50	66.94	2054	672	2248	1987

(1976; Leg 33). Sites having the highest sedimentation rates also have the highest variations in interstitial water composition.

The relationship between the rate of sedimentation and the chemistry of the carbonates appears to be more complex. In Hole 549 the average Sr concentration for any given sediment interval has no direct relationship to the corresponding sedimentation rate. An inverse correlation exists, however, between the cumulative sedimentation rate (Fig. 3) and the Sr concentration, at least for the Paleocene–Miocene time interval. This negative correlation does not hold for the Cretaceous sediments. This means that either the diagenetic process or the chemistry of the ocean water was different in the Cretaceous. To go further with this analysis, we have made a comparison of these results with those obtained for Hole 400A (Renard, Létolle, et al., 1979). In contrast to Site 549, this site is characterized by a substantial accumulation of post-Oligocene sediments. Consequently, curves of chemical evolution of interstitial waters through time are different for these two sites (Fig. 2). The Sr/Ca ratio for water is about 8×10^{-2} at 100 m depth in Hole 400A (Pliocene) and about 1.4×10^{-2} at 100 m depth (Oligocene) in Hole 549. The difference, however, diminishes with depth: the Sr/Ca ratio is 3×10^{-2} at 500 m depth (Eocene) for Hole 400A and 1×10^{-2} for Hole 549 (Cretaceous).

Note the plot of Sr content versus cumulative sedimentation rate for Holes 400A and 549 in Figure 3. The plot of Hole 400A varies in a nearly opposite manner from that of Hole 549. This "antithetic" behavior implies that the rate of sedimentation for Sr is not the main factor controlling diagenesis.

Overall both sites display a similar decrease in Sr content with increasing age of sediments (Figs. 2 and 3). The average values from Hole 400A, however, are always higher than those from Hole 549, with the difference gradually diminishing with the age of the sediments. Carbonates from Hole 400A show the largest amplitude of variation in the Sr/Ca ratio of interstitial waters and the highest Sr content in sediments, whereas Hole 549 shows the lowest Sr content in carbonate and also shows less variation in the Sr/Ca ratio of interstitial waters. Hole 116 is intermediate between the two, especially for the plots of interstitial waters.

It is thus possible that the rate of sedimentation controls the amplitude of the chemical variations in the interstitial waters. The Sr/Ca ratio is close to seawater values for sites with low sedimentation rates but exceeds this ratio for sites with high sedimentation rates. In contrast, the rate of diagenetic transformation of sediments is apparently controlled by their age or, more exactly, the residence time of sediments in a given diagenetic environment.

During dissolution and recrystallization, the newly formed calcite attains equilibrium with its diagenetic environment. Note, however, that the difference in Sr content of sediments among different sites is only ~20%, whereas the difference in Sr content of interstitial waters is ~80%. This implies that $K_{Sr}^{calcite}$ during the transformation of low-Mg calcite to low-Mg calcite is considerably less than the equilibrium constant corresponding to inorganic precipitations ($K_{Sr} = 0.14$ at 25°C [Kinsman, 1969]). The K_{Sr} value of 0.04 (Katz et al., 1972; Baker et al., 1982) determined from aragonite–calcite transformations seems more appropriate for our use.

Magnesium

The variation in Mg content of sediments from Hole 549 are more complex than those of Sr. There is an increase from 1300 to 3250 ppm with increasing depth and age for the late Miocene to late Paleocene interval (Fig. 1). This is inverse to the change in Sr over the same interval; a similar inverse relationship has been observed at Site 116 and in the Gubbio section outcrop.

A break in the Mg content curve for upper Paleocene to Maestrichtian sediments is followed by another increasing trend from 1200 ppm in the Maestrichtian section to 6000 ppm in the Albian section. The evolution of

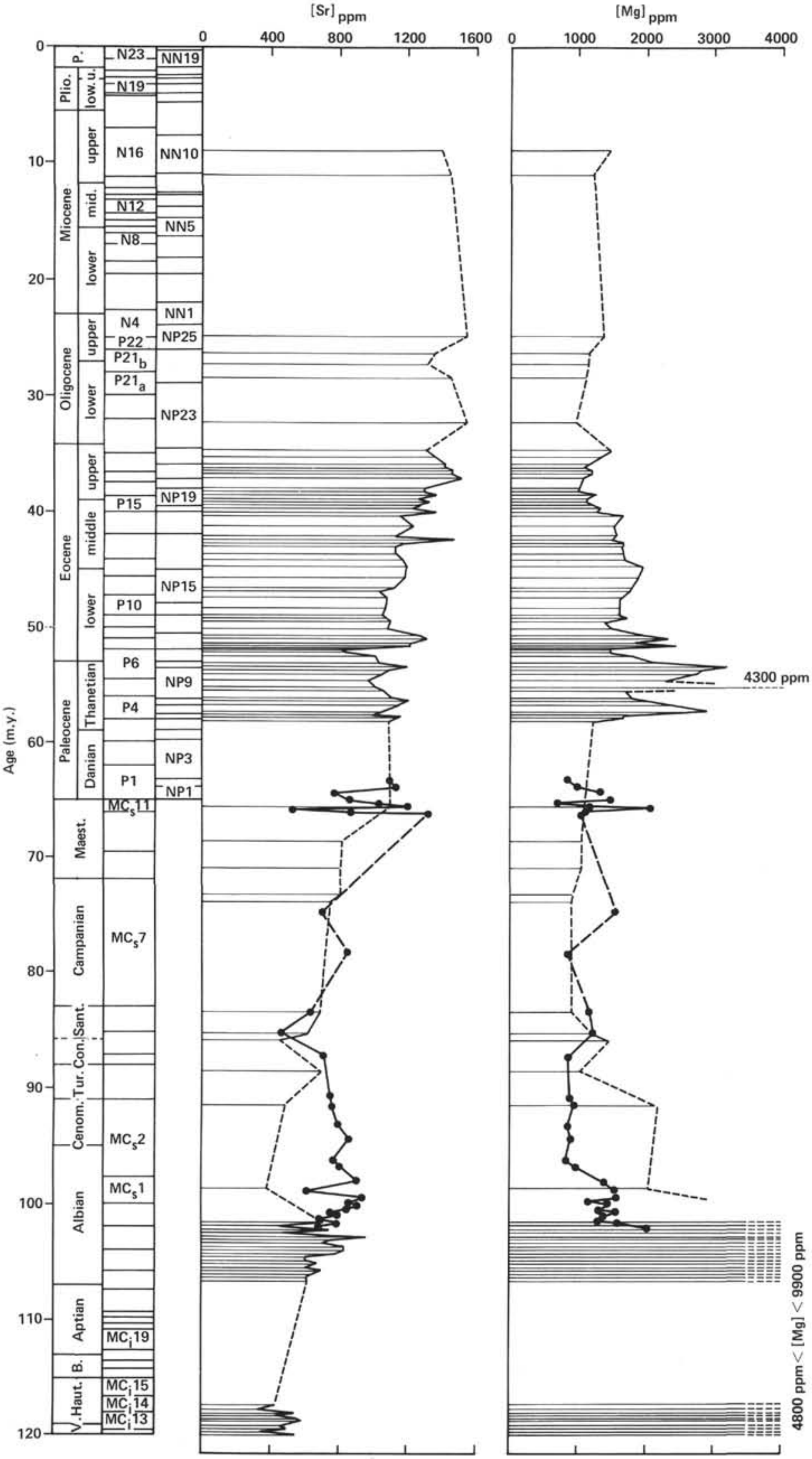

Figure 1. Sr, Mg, Mn, and Fe concentration curves related to sediment age in Holes 549 and 550B. Biostratigraphy is from Snyder et al. (this volume). Absolute age dating is from Odin (1981). Dashed line denotes intervals where profile is uncertain or unknown because of scarcity or absence of data.

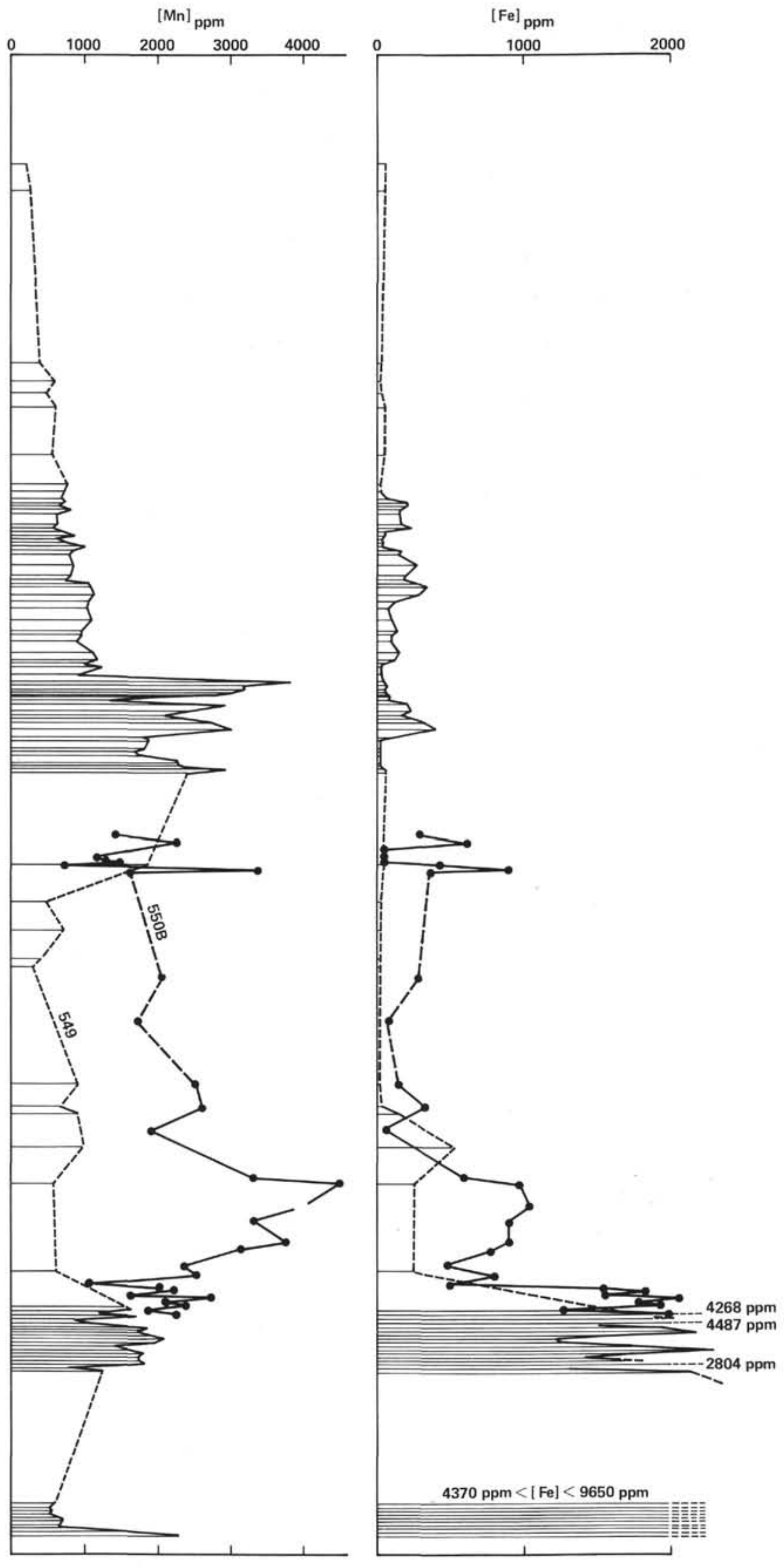

Figure 1. (Continued).

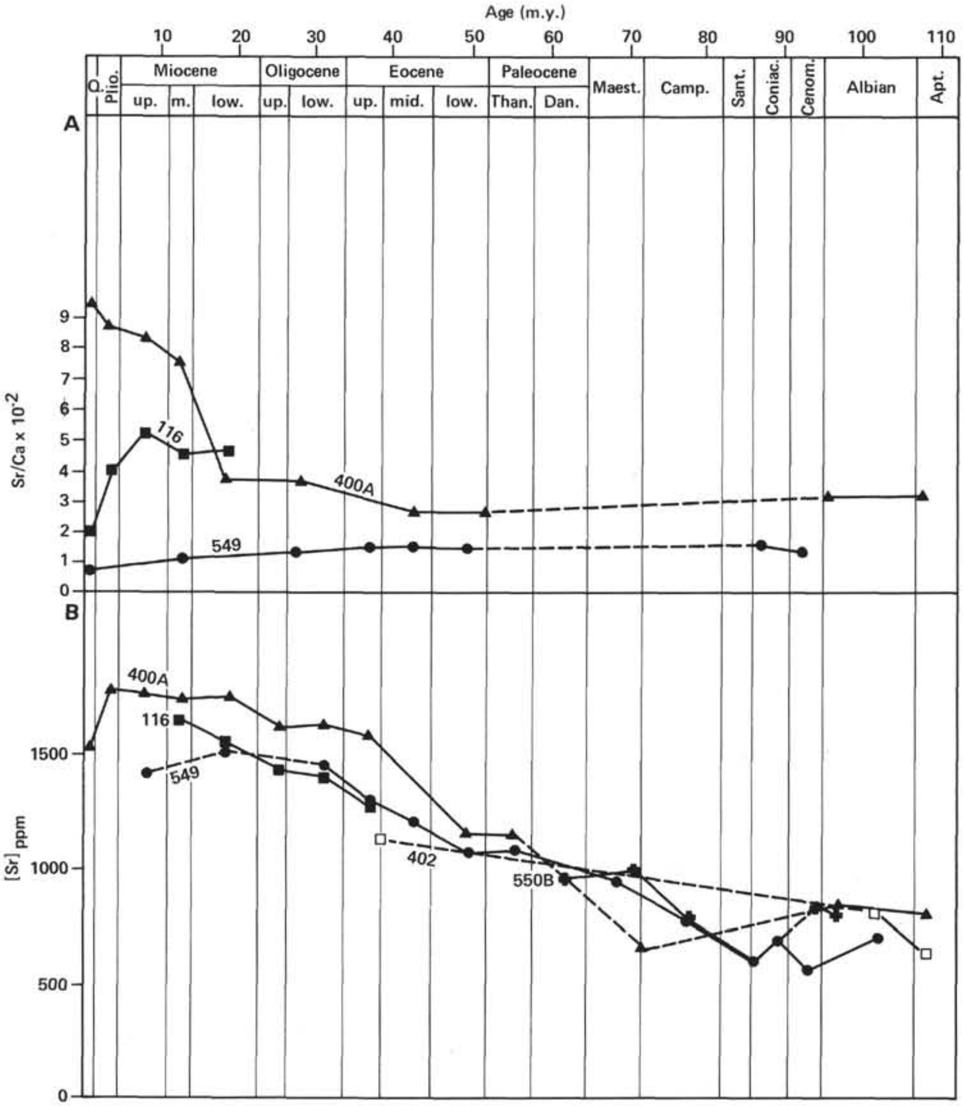

Figure 2. A. Evolution of Sr/Ca ratio in interstitial water as related to sediment age for the North Atlantic sites. B. Sr contents of sediments related to age for the same sites. Dashed line as in Fig. 1.

Mg concentration of the interstitial waters, at least for the post-Paleocene interval, is inversely related to that of the sediments (Gieskes, this volume); Mg concentrations range from 1300 ppm (Pleistocene) to 1000 ppm (upper Paleocene). The Mg/Ca ratio (Fig. 4) for the interstitial waters from Pleistocene to mid-Cretaceous sediments decreases as well. During diagenesis, the newly formed calcite must have been enriched in Mg at the expense of the interstitial waters. However, the Mg decrease may not only be caused by carbonate diagenesis but also by the alteration of volcanic materials (Elderfield et al., 1982).

The influence of the sedimentation rate from a given age appears to be more important for Mg than for Sr because Mg shows relatively good positive correlation with the log of the sedimentation rate (Fig. 5). Consequently, the low-Mg content of Upper Cretaceous sediments may be linked to a particularly low sedimentation rate.

The Mg content of the Upper Cretaceous sediments in Hole 550B is close to that observed in Hole 549 (Fig. 1) and similar to that found in the Gubbio section outcrop (Fig. 4). In contrast, the Tertiary sediments from Gubbio, Hole 549, and Hole 116 have different Mg concentrations. There are particularly notable differences between the Thanetian values from Gubbio and Hole 549. These differences disappear, at least in the Tertiary sections, if the plot of Mg concentration versus the apparent rate of sedimentation is considered (Fig. 4). But a difference persists between Site 116 and Site 549 for the Oligocene to Miocene interval. Because of the existence of numerous hiatuses at Sites 549 and 550, which make the calculation of sedimentation rates uncertain, we have not investigated the ratio of Mg concentration to sedimentation rate for Cretaceous sediments.

Samples from Site 549 show a negative Sr/Mg relationship (Fig. 6) characteristic of the diagenesis of pelagic carbonates. It appears that Mg diagenesis is a rel-

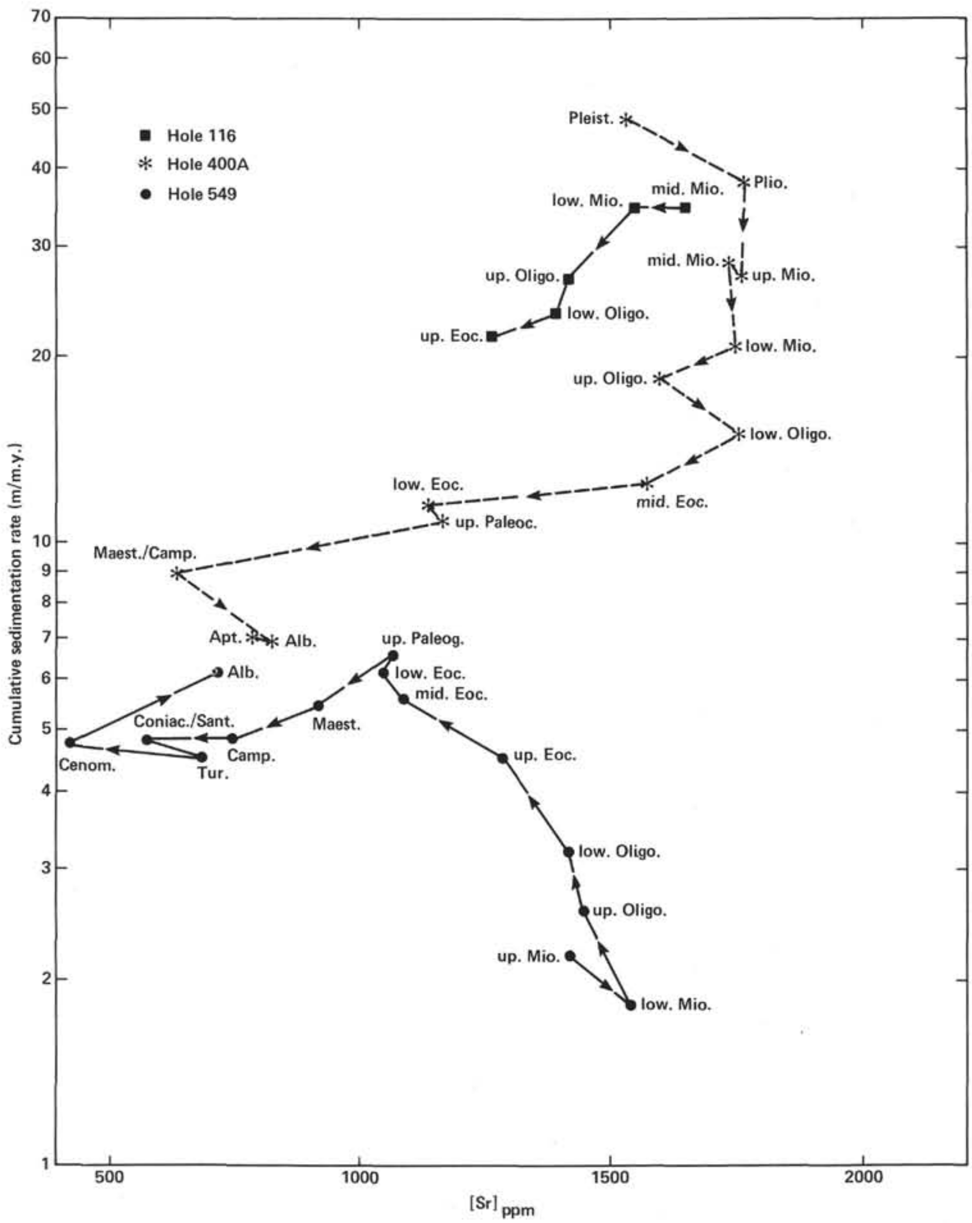

Figure 3. Relationship between the log of cumulative sedimentation rate and Sr concentration for Holes 116, 400A, and 549.

atively fast process and is thus sensitive to the sedimentation rate of each individual interval; in contrast, Sr diagenesis is a long-term phenomenon and is thus sensitive to the overall sedimentation rate at each site. This agrees with numerous previous observations (Lorens et al., 1977; Walls et al., 1977) of biogenic carbonates which have shown that a substantial amount of Mg is exchangeable and is thus very sensitive to dissolution phenomena and to early diagenesis.

We have noticed a break in the slope of Sr and Mg curves for the Paleocene interval, particularly for Mg at Site 549 (Fig. 4). This break may be the result of variations in sedimentation rates or of variations in seawater chemistry during Danian time. New results show that the Sr/Ca and Mg/Ca ratios of seawater changed during the Cenozoic (Graham et al., 1982) and Mesozoic (Renard, in press).

Manganese

The distribution curve for Hole 549 (Fig. 1) is not regular. Certain intervals, such as Albian (750–2000 ppm) and upper Paleocene to lower Miocene, are rich in Mn (1250–3750 ppm), and others, notably middle to Upper Cretaceous, are depleted in Mn (250–1250 ppm).

The sediments in Hole 550B, which lie on oceanic crust, shows systematically higher values than Hole 549. However, this hole contains Mn-rich intervals (Albian–Cenomanian; 100–4500 ppm) and Mn-poor intervals (Late Cretaceous–lower Paleocene, 750–2500 ppm).

It is now well established (Bostrom and Peterson, 1966; Klinkhammer, 1980) that the source of Mn in the ocean is mainly volcano-hydrothermal activity. In our previous publications (Renard, Létolle, et al., 1979; Rénard, Richebois, et al., 1979), we have shown the poten-

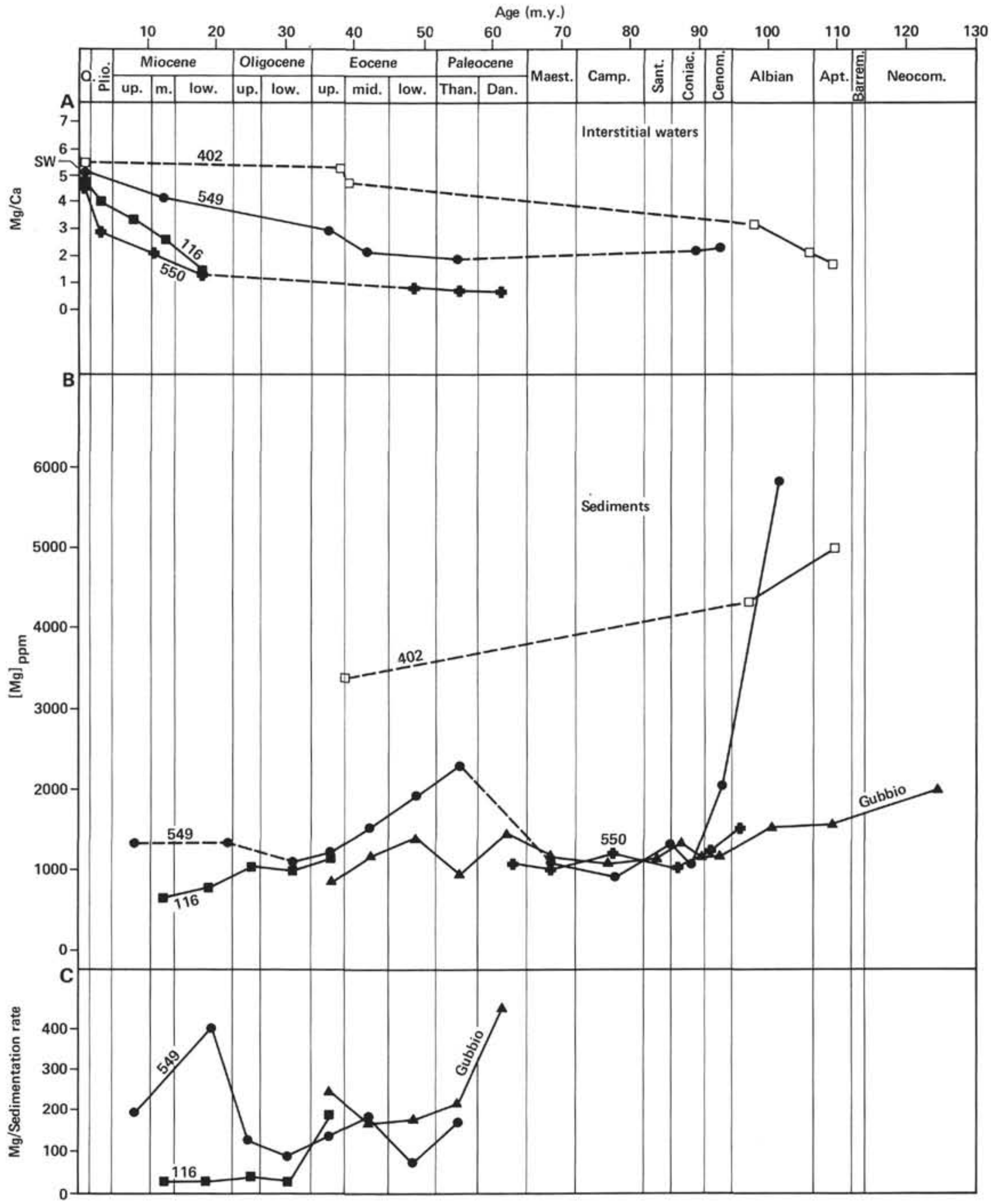

Figure 4. A. Evolution of Mg/Ca in interstitial waters related to the age of sediments for the North Atlantic sites. B. Average Mg content of sediments related to their age for the same sites and for Gubbio section outcrop (Italy). C. Mg versus apparent sedimentation rate for the Tertiary sediments in the DSDP holes and for the Gubbio section outcrop. Dashed line as in Fig. 1.

tial use of Mn and Fe as time markers for the main seafloor spreading periods and as stratigraphic correlation tools (Odin et al., 1982).

The theoretical behavior of Mn during carbonate sedimentation is well known (Michard, 1969). Precipitation of Mn is controlled by two main phenomena:

1. Coprecipitation with calcite $(Ca_{(1-x)}Mn_x)CO_3$ ($x \ll 1$). Because of low Mn concentration in seawater and because $K_{Mn}{}^{inorg} = 5.4 \pm 0.3$, these carbonates are impoverished in Mn (5 ppm < Mn ≤ 55 ppm).

2. Precipitation of MnO_2 when redox conditions of the environment are favorable. If Mn-poor biogenic calcites that fall on the seafloor stay long enough in the oxidizing layer of sediments, the precipitation of oxides (catalyzed by carbonates), such as ferric oxides and MnO_2, leads to an increase in the Mn content of the sediments, but this Mn is not in the lattice of calcites.

The present Mn concentration values are compared with those from other North Atlantic DSDP holes, such as 116 (Rabussier, 1980), 390, 392 (Renard et al., 1978),

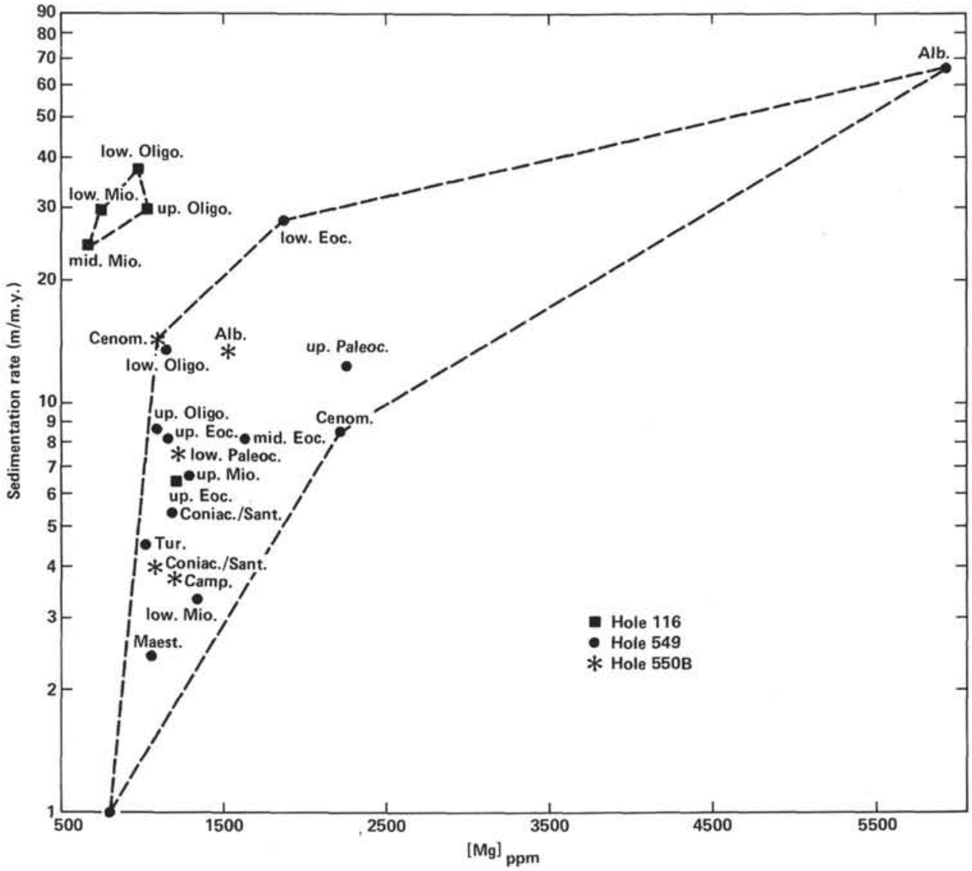

Figure 5. Relationship between the logarithm of sedimentation rates and Mg concentrations for Holes 116, 549, and 550B.

398 (Renard, Richebois et al., 1979), 400A, 401, and 402A (Renard, Létolle, et al., 1979; Andrianiazy, 1983). The sediments sampled in these holes represent a large variety of environments, in terms of depth, latitude, and type of substratum. We attempted to determine the role of these factors on Fe and Mn contents of pelagic carbonates.

Mn Contents of North Atlantic Pelagic Carbonates: Evolution and Influence of Mid-Atlantic Ridge Activity

The composite curves of Mn distribution show overall similarities among the sites (Fig. 7). We found Mn-rich intervals (Albian and upper Paleocene to middle Eocene) and Mn-poor intervals (Upper Cretaceous and upper Oligocene to Holocene), already described in Figure 1 for Sites 549 and 550. There appears to be good correlation between Mn-rich periods and the main geodynamic events of the oceanic basin. The Albian was the main period of spreading in the Bay of Biscay (Williams, 1975) and the beginning of Mid-Atlantic Ridge activity in the Goban Spur area. Late Paleocene to middle Eocene time was the most active period in the opening history of the North Atlantic ocean. During this time, spreading began in the Reykjanes Ridge area, separating Rockall Plateau from Greenland (Roberts et al., 1979; Olivet et al., 1981).

There is a strong parallelism between the history of North Atlantic spreading (LePichon, 1968) and the evolution of Mn contents in pelagic sediments. During Aptian–Albian time, active rifting (beginning 120 m.y. ago) was followed by an episode of rapid spreading lasting about 30 m.y.; carbonate sediments of this time show very high Mn contents. This episode seems to have stopped during the mid-Cretaceous, and the Mn concentration decreased as well. During Late Cretaceous time, the spreading rate decreased notably and approached zero. Thus, we find very low Mn values in upper Maestrichtian and lower Paleocene sediments. During Paleocene time, spreading started again, extending northward to the Labrador Sea, Norway Sea, and Arctic Sea, correlating again with high Mn contents. Also during this period important volcanic activity occurred in northwestern Europe, the North Sea, and the North Atlantic Ocean, as confirmed by the presence of volcanic glass and tuff in the sediments (Harrison et al., 1979). From Oligocene to Miocene time, the spreading rate decreased again and probably stopped; this period corresponds to low-Mn contents. From late Miocene time, a new spreading cycle seems to have begun again but with a very slow rate. These numerous coincidences lead us to postulate that the variations in seafloor geodynamic activity correspond to variations of volcano-hydrothermal activity

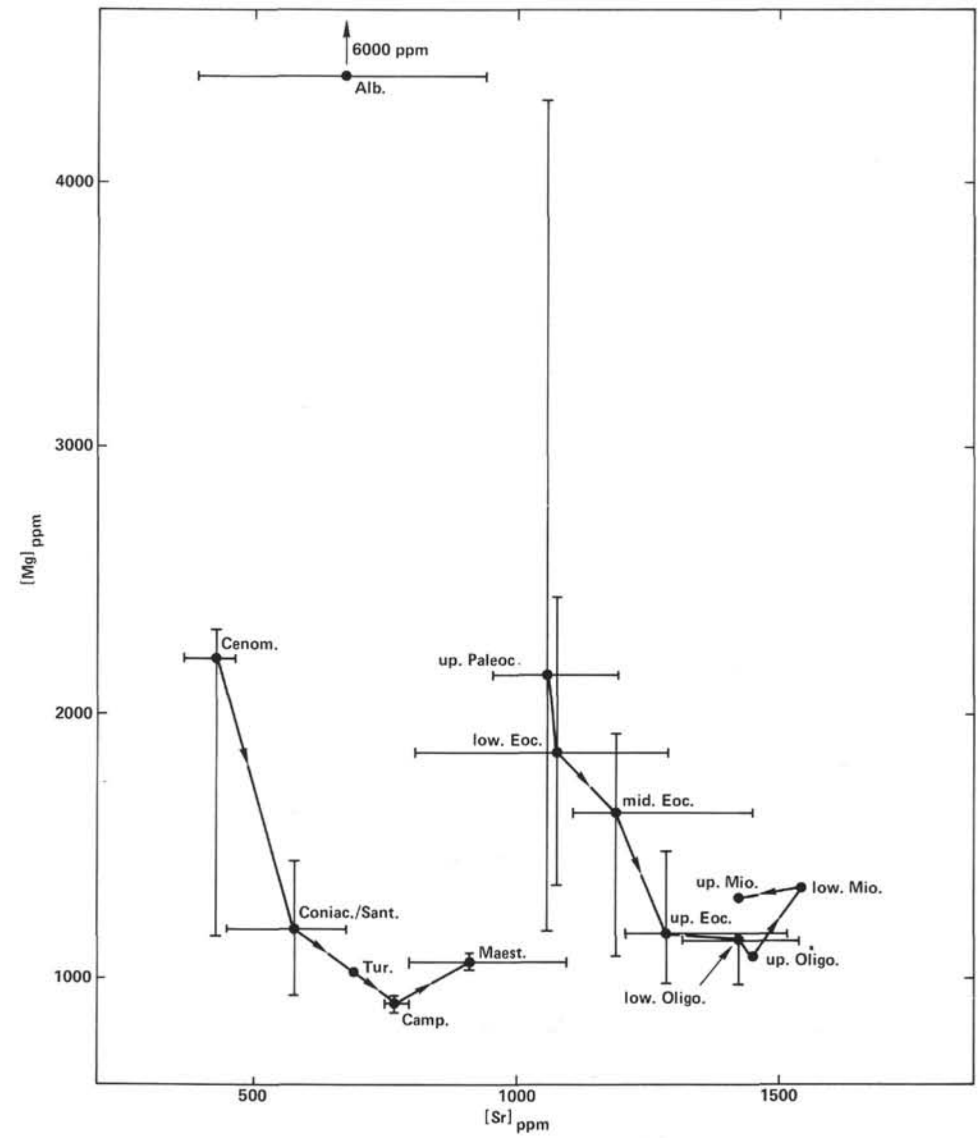

Figure 6. Relationship between average Mg and Sr concentrations in Hole 549 sediments.

on the ridges. Such variations are recorded by pelagic carbonates through fluctuations in Mn concentration.

Influences of Paleodepth on Mn Concentrations: Role of Carbonate Dissolution

Even if the relationship between mid-ocean ridge activity and Mn concentrations in pelagic carbonates seems well established, it is not as simple as our previous studies led us to believe. First of all, the differences in average Mn concentrations for fast-spreading versus slow-spreading periods are too large to be explained solely by differences in ridge activity. Second, Mn concentrations in sediments of the same age are very different from one site to another. For instance, for middle and upper Eocene sediments, the average concentrations are 4500 ppm for Hole 400A, 3000 ppm for Hole 398, 1355 ppm for Hole 401, 900 ppm for Hole 549, and 600 ppm for Hole 402A.

These variations are not attributable to the distances from the ridge during Eocene time. For example, during the early Eocene, Holes 400A and 398 were at approximately the same distance from the ridge (about 610 and 590 km, respectively), whereas Hole 549 was closer (about 330 km).

Moreover, there is no clear relationship between the Mn concentrations of a period and the corresponding sedimentation rate. Thus, the theoretical model based on the sedimentation rate being the sole factor controlling the Mn concentration is not applicable; however, as we shall see later, the sedimentation rate does play a role in Mn distribution.

Overall, there is a strong positive correlation between the log of the Mn content and the depth at which the sediments were deposited. Figure 8 shows for each site the evolution of the average Mn content related to the depth and, for each period, the correlation curves: $\log[Mn]_{ppm} = f\,(\text{paleodepth})_m$. The equations are

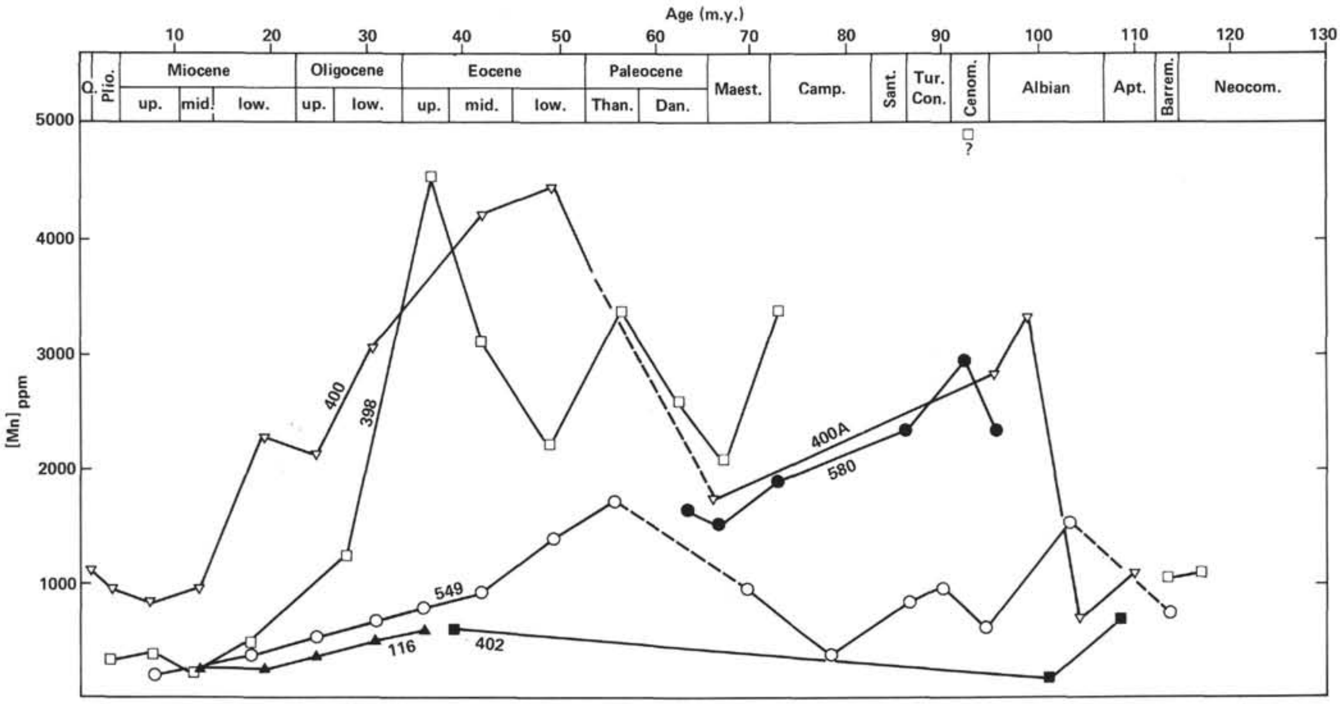

Figure 7. Evolution of average Mn concentrations versus age at the North Atlantic sites. Dashed line as in Fig. 1.

for Albian (correlation is calculated without including Hole 549, r = 0.986):

$$\log[Mn]_{ppm} = 7.85 \times 10^{-4} (\text{depth})_m + 1.63$$

for Maestrichtian (r = 0.855):

$$\log[Mn]_{ppm} = 2.67 \times 10^{-4} (\text{depth})_m + 2.39$$

for middle-upper Eocene (correlation is calculated without including Hole 116, r = 0.905):

$$\log[Mn]_{ppm} = 4.84 \times 10^{-4} (\text{depth})_m + 1.73$$

for upper Oligocene (r = 0.984):

$$\log[Mn]_{ppm} = 2.19 \times 10^{-4} (\text{depth})_m + 2.31$$

for upper Miocene (r = 0.826):

$$\log[Mn]_{ppm} = 1.92 \times 10^{-4} (\text{depth})_m + 1.96$$

The depth of deposition seems to be the determinative factor of Mn variability from one site to another. The ridge activity appears to be the factor which partially explains the variations between different periods. In fact, these influences are complementary, although one factor may be dominant at any one time. This happens, for example, at the onset of seafloor spreading. Albian sediments from Hole 549, although deposited in a shallow water environment (−250 m), are Mn rich because this site was close to the ridge. For this reason we do not take them into account for the correlation calculation. The same circumstances apparently existed during late Eocene at Site 116. The nature of the substratum, whether oceanic or continental, did not seem to play a role in the Mn distribution. The differences observed between Mn contents from Hole 549 (continental crust) and from Hole 550B (oceanic crust) are more a function of depth than of the nature of the substratum.

Correlation curves of the log of Mn contents versus depth (Fig. 8) are similar during supposed periods of low ridge activity (Maestrichtian, late Oligocene, and late Miocene) (slope lower than 3×10^{-4} and the origin on the ordinate higher than 1.96 [90 ppm]) and during periods of very high ridge activity (Albian-middle Eocene) (slope higher than 4.5×10^{-4} and the origin on the ordinate lower than 1.73 [54 ppm]). This means that the greater the Mn production from the ridge, the more intense the influence of paleodepth on Mn concentrations.

This relationship leads us to consider the problem of the $CaCO_3$ concentration. Because of the increasing dissolution of carbonates with depth, the dilution of Mn by calcareous biogenic sedimentation becomes less important with depth. In fact, numerous sites show a negative correlation between Mn and $CaCO_3$ (Fig. 9). Sediments of Albian age do not conform to this correlation. Although depleted in $CaCO_3$, sediments from Holes 549, 550B, and 400A are only moderately rich in Mn. Similarly, samples of Miocene, Pliocene, and Pleistocene sediments from Hole 400A are relatively low in $CaCO_3$ (45–65%) but have low Mn concentrations resulting from low production of Mn during these periods. In contrast, because of high Mn production during Cenomanian time, the sediments from Hole 398 are rich in Mn despite their similar $CaCO_3$ contents (55%).

The study of correlation coefficients shows that this negative relationship between Mn and $CaCO_3$ is strong only for post–Upper Cretaceous sediments (Fig. 9).

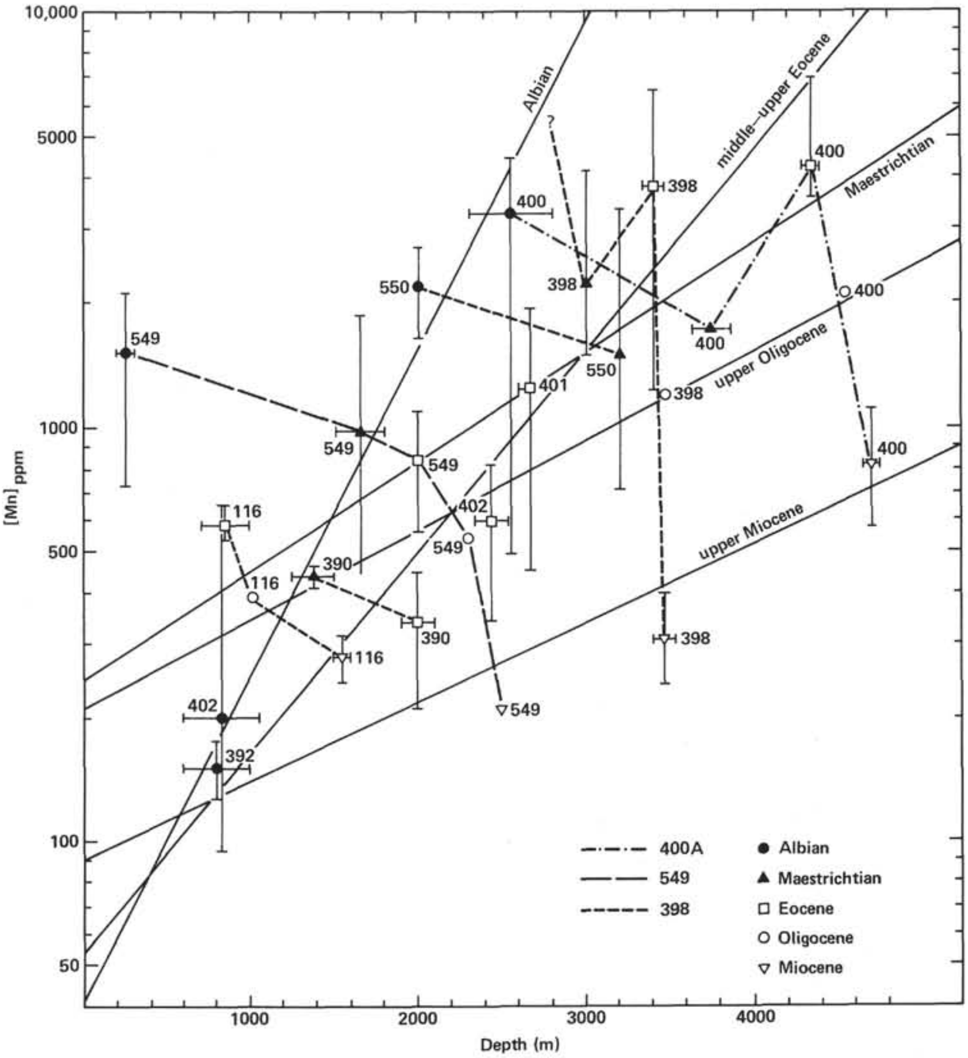

Figure 8. Relationship between the logarithm of Mn average contents and the depth during the Albian, Maestrichtian, Eocene, late Oligocene, and late Miocene. (Depths for Holes 549 and 550 are from site chapters, this volume.)

For the five test periods the calculation of correlation coefficient gives $r = -0.07$ for Albian, $r = -0.62$ for Maestrichtian, $r = -0.81$ for Eocene, $r = -0.99$ for Oligocene, and $r = -0.93$ for Miocene.

Therefore, for Eocene time, which is characterized by low $CaCO_3$ content in all North Atlantic sites, is this Mn enrichment real or is it just a result of the low carbonate content? These two phenomena, in fact, are not completely independent: intense volcano-hydrothermal activity at the ridge could acidify the seawater and thus favor carbonate dissolution. (This could explain the steeper slope of the Eocene curve of $\log[Mn] = f(\text{depth})$ in Fig. 8.) To eliminate the problem of differential dilution of Mn by biogenic carbonates, we have recalculated the Mn concentrations with respect to 100% carbonate. We can define $[Mn]^{100}$ as the concentration of Mn corrected by carbonate percentage:

$$[Mn]^{100} = \frac{[Mn]_{ppm} \times [CaCO_3]_{\%}}{100}$$

Using this recalculated $[Mn]^{100}$ value, a new plot was made (Fig. 10). From this plot, we can make the following observations:

1. The differences in Mn concentrations for various sites are diminished, particularly for the post–Upper Cretaceous sediments.

2. The curves are more parallel and synchronous than before the treatment, particularly for Holes 400 and 398.

3. The recalculation has diminished the differences between high and low periods of concentrations, but it has not completely erased them. Thus, these differences are apparently not attributable solely to carbonate dilution. Furthermore, the Mn concentration curves do not follow the carbonate compensation depth (CCD) curve. Thus, the high- and low-Mn periods are real. In Cenomanian–Maestrichtian and lower Paleocene sediments, one can observe a continuous decrease of $[Mn]^{100}$ (Sites 398 and 550). This is followed by an increase in the upper Paleocene and lower Eocene interval. From the mid-

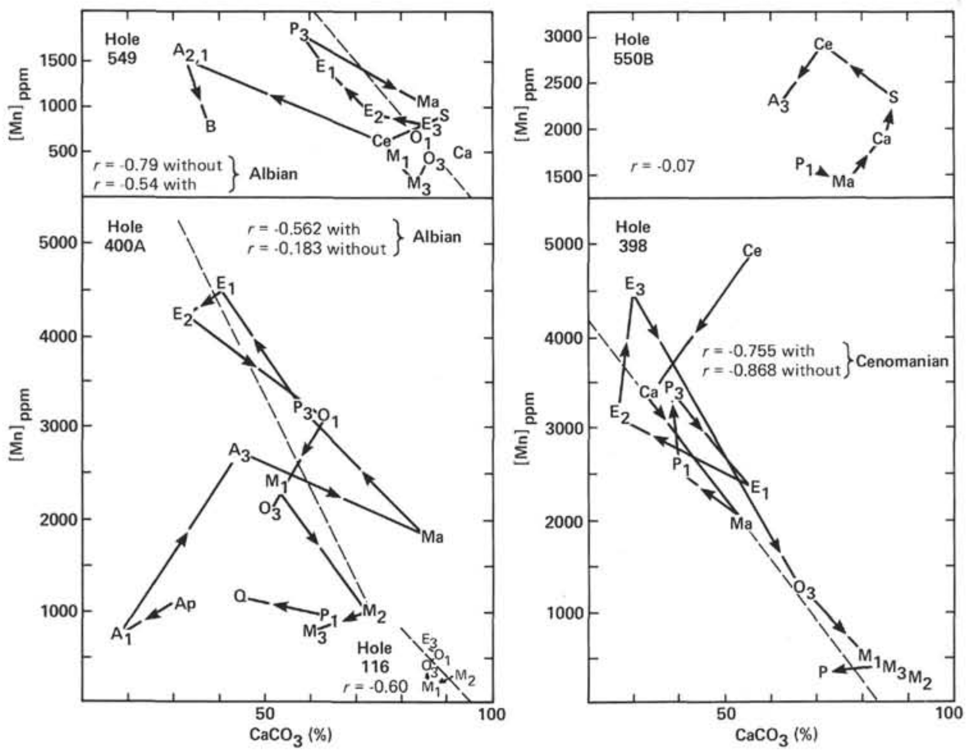

Figure 9. Relationship between average $CaCO_3$ and Mn contents in sediments from Holes 116, 398, 400A, 549, and 550B. Dashed line denotes correlation line. Q = Quaternary, P = Pleistocene, M = Miocene, O = Oligocene, E = Eocene, P_1 or P_3 = Paleocene, Ma = Maestrichtian, Ca = Campanian, S = Santonian, Ce = Cenomanian, A = Albian, Ap = Aptian, B = Barremian; 1 = early, 2 = middle, 3 = late.

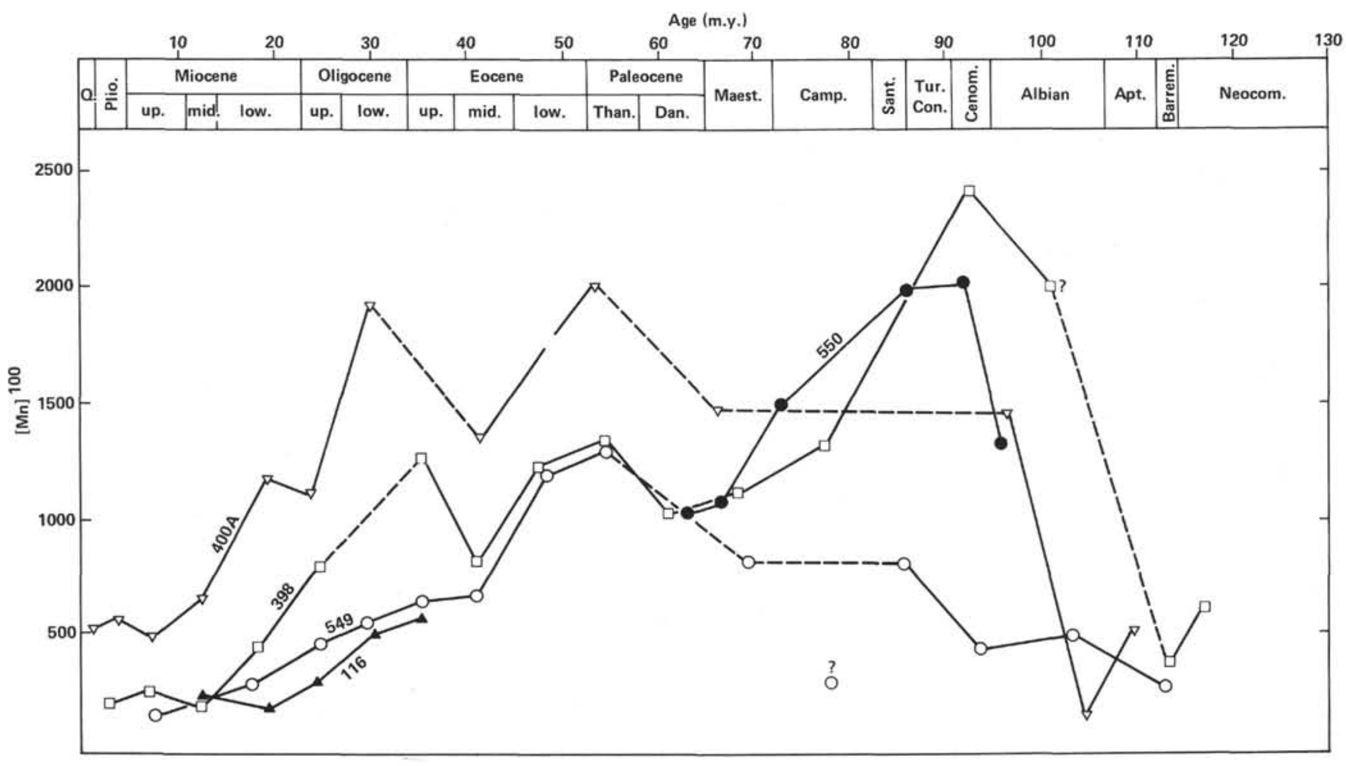

Figure 10. Evolution of $[Mn]^{100}$ ($[Mn]_{ppm} \times$ % $CaCO_3/100$) in Lower Cretaceous to Pleistocene pelagic carbonates from the North Atlantic sites.

dle Eocene section upward, a general decrease can be seen (Sites 400, 398, and 549) but two cases should be distinguished (Fig. 10). At the northern sites (549–116), concentrations of Mn^{100} decrease regularly from the upper Eocene to the present, but the decrease becomes steeper in the Oligocene interval in Site 116. Also, at the midlatitude sites (400 and 398), one can see an increase of Mn^{100} values in the upper Eocene and lower Oligocene sections, followed by the same decrease as seen at northern sites. Because Sites 400 and 398 are the deepest ones, two explanations are possible. Either this was a local phenomenon (submarine volcanism?), or it was more widespread but oceanic conditions were such that only deep sites actually recorded it.

4. From Maestrichtian to the present, the $[Mn]^{100}$ curve for Site 549 is similar to that for other sites, except for the mid-Cretaceous. We shall explain this observation later.

Role of the Redox Conditions

Is the relationship between log[Mn] and depth only a result of the variation in $CaCO_3$? This is not likely because the observed relationship between $[Mn]^{100}$ and the depth confirm their correlation. A plot of $\log[Mn]^{100}$ versus depth for the five test periods gives the following correlation curves (Fig. 11):

Albian (not including Hole 549, r = 0.972; including Hole 549, r = 0.702):

$$\log[Mn]^{100}_{ppm} = 7.95 \times 10^{-4}\,(\text{depth})_m + 1.32$$

Maestrichtian (r = 0.873):

$$\log[Mn]^{100}_{ppm} = 2.37 \times 10^{-4}\,(\text{depth})_m + 2.35$$

middle–upper Eocene (not including Hole 116, r = 0.797):

$$\log[Mn]^{100}_{ppm} = 3.05 \times 10^{-4}\,(\text{depth})_m + 1.94$$

upper Oligocene (r = 0.993):

$$\log[Mn]^{100}_{ppm} = 1.52 \times 10^{-4}\,(\text{depth})_m + 2.36$$

upper Miocene (r = 0.75):

$$\log[Mn]^{100}_{ppm} = 1.41 \times 10^{-4}\,(\text{depth})_m + 2.01$$

By comparison of these curves with those in Figure 8, the following observations can be made:

1. The correction did not modify the curve for the Albian section (Figs. 8 and 11), which is different from the other curves.

2. The correction has only slightly modified the curves for Maestrichtian, upper Oligocene, and upper Miocene sediments.

3. The modification is more important for the curve for the Eocene sediments, and its slope (although steep) is close to that for Maestrichtian, Oligocene, and Miocene sediments. Consequently, the Eocene interval shows a higher gradient of carbonate dissolution with depth than that of the Maestrichtian, Oligocene, and Miocene.

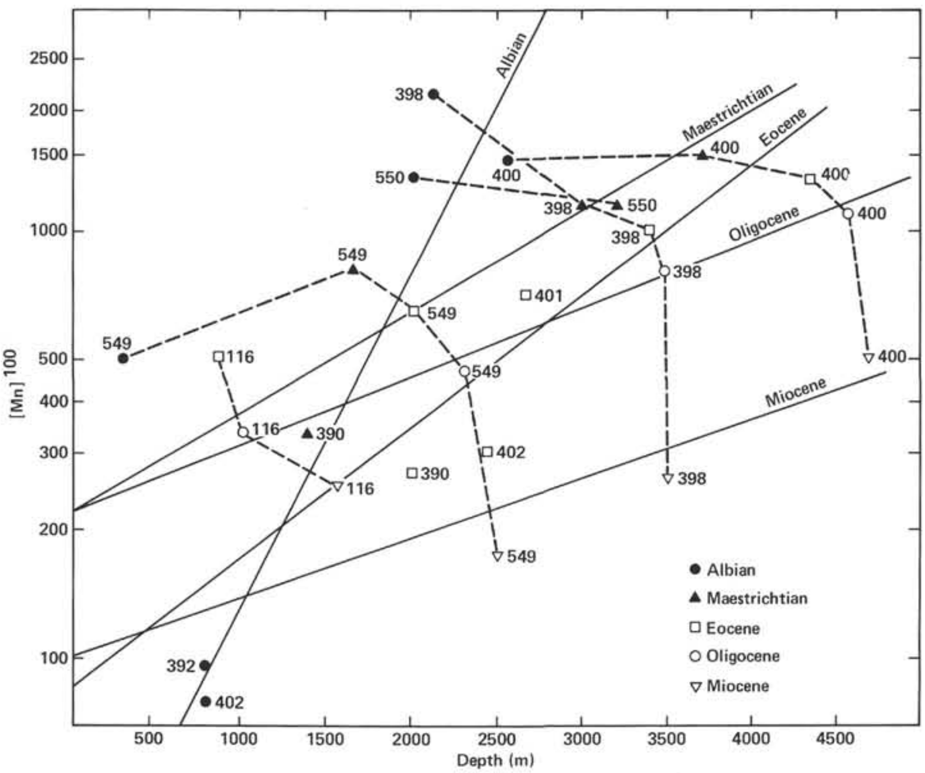

Figure 11. Relationship between the logarithm of $[Mn]^{100}$ (defined in Fig. 10) and the depth of the site for the five test periods.

Two other observations should be considered:

1. The post-Cretaceous sediments show a positive correlation between the slope of the curve of $\log[Mn]^{100} = f(\text{depth})$ and the percentage of the hiatus (Doche, 1976) observed in North Atlantic holes drilled in sediments of the same age (Fig. 12). Although we do not have an exact compilation, it seems that the hiatus frequency for Albian time is very low and that the correlation does not hold. The existence of this correlation for the post-Cretaceous is important because the presence of a hiatus is partly the result of erosion by well-oxidized deep waters (Rabussier, 1980).

2. For any given age, an inverse exponential relationship exists between the slope of the curve of $\log[Mn]^{100} = f(\text{depth})$ and the sedimentation rate (Fig. 13). This correlation does not hold for the Albian. The lower the sedimentation rate, the higher the Mn content of pelagic carbonates because the residence time of precipitated calcite in the oxidizing layer of sediments is correspondingly longer.

These two observations lead us to believe that redox conditions of the medium play a role in the influence of depth on variations of Mn concentration in sediments. As one moves downward from the oxygen minimum layer, oxygen increases (Kroopnick et al., 1972), and the presence of oxygenated bottom water makes it easier to precipitate MnO_2. It seems that the late Paleocene and Eocene, which were periods when Mn production by the ridge was important, were also times when the environment was the most suitable for the precipitation of Mn. During certain past geologic times, the oxygen minimum layer has gone through periods of expansion and contraction. Aptian to Albian time seems to have been a period with a particularly well-developed oxygen minimum layer (i.e., an anoxic period) (Fischer and Arthur, 1977). During this time, the seafloor of the North Atlantic began to spread and was very confined. During

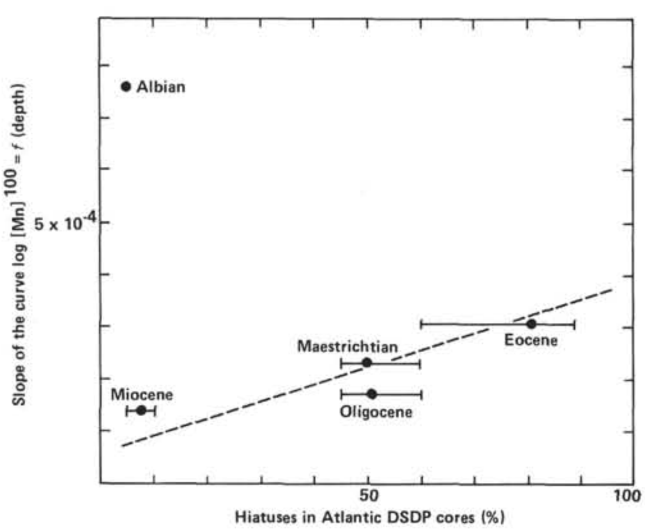

Figure 12. Relationship between the slope of the curve $\log [Mn]^{100} = f(\text{depth})$ and the observed percentage of hiatuses for each test period. Dashed line denotes correlation line.

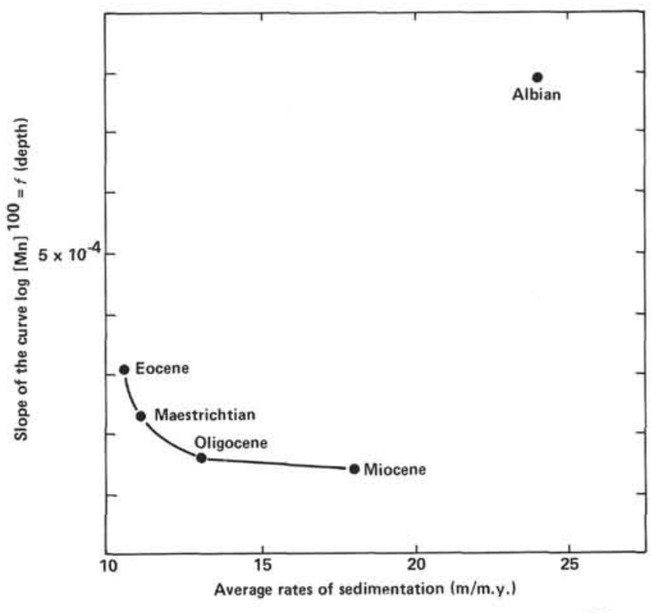

Figure 13. Relationship between the slope of the curve $\log [Mn]^{100} = f(\text{depth})$ and the average sedimentation rate for each test period.

these anoxic conditions, MnO_2 could not easily precipitate. This leads us to postulate that Mn production by the mid-ocean ridge was more important during Albian time than during Eocene time. This pattern would also explain the low-Mn content of sediments in Hole 549 because this site was shallow and close to the oxygen minimum layer in the past.

Influence of the Distance from the Ridge

There is a strong negative correlation between the log of the $[Mn]^{100}$/depth ratio and the distance from the ridge (Fig. 14). This means that after correction for the role of carbonate dilution and for depth, the distance from the ridge is apparently the controlling factor of Mn distribution in sediments. The equation ($r = 0.70$) is

$$\log([Mn]^{100}/\text{depth}) = -1.003 \times 10^{-3} \text{ (distance to ridge)} + 3.06$$

where the distance to the ridge is in km.

In conclusion, Mn distribution in pelagic sediments appears to depend on three factors: (1) the activity of the ridge, (2) the depth, which controls carbonate dissolution and seafloor oxygenation, and (3) the distance from the ridge.

Iron

As in the case of Mn (Fig. 1), Fe distribution curves are not regular. In Hole 549, Albian and mid-Cretaceous sediments are Fe rich (1250–6500 ppm), whereas Upper Cretaceous and lower Paleocene sediments are impoverished in Fe (10–50 ppm). Upper Paleocene to upper Eocene carbonates are moderately enriched (100–380 ppm). From lower Oligocene to present sediments, the concentrations are low (10–50 ppm). Comparison of this distribution to that of Mn shows that their variations correlate. However, Albian is more enriched in Fe

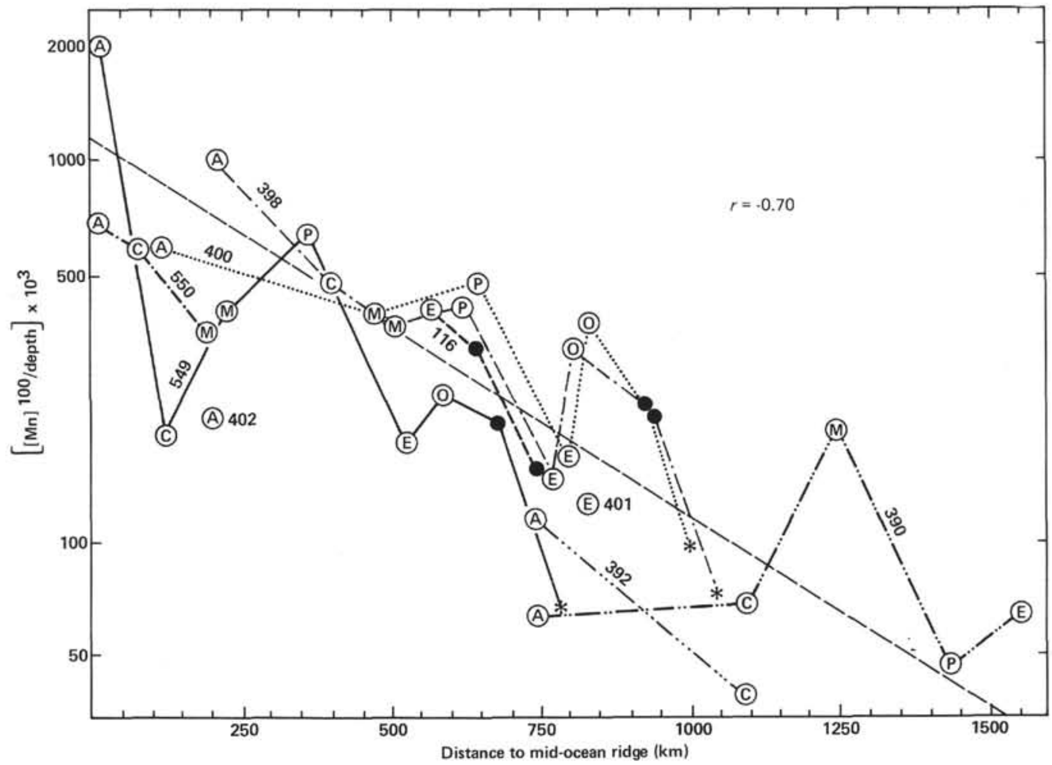

Figure 14. Relationship between the log of average $[Mn]^{100}$ content versus depth and distance from the ancient mid-ocean ridge for each site. Even dashes denote correlation line. A = Albian; C = Cenomanian; M = Maestrichtian; P = Paleocene; E = Eocene; O = Oligocene; ● = Miocene; * = Quaternary.

than Mn. In contrast, upper Paleocene and Eocene sediments are more enriched in Mn than in Fe.

As already demonstrated for Mn, Fe concentrations are systematically higher in Hole 550 than in Hole 549 (500–2050 ppm for the upper Albian and mid-Cretaceous sediments).

The curves of average Fe concentrations for several North Atlantic sites (Fig. 15) seem to be more complex than those for Mn, but again a general Albian–Cenomanian enrichment can be observed at all sites. Whereas all sites show high-Mn concentrations, only Site 116 (close to the ridge) shows an enrichment in Fe. This distribution is a result of the difference in the chemical behavior of Mn and Fe. Iron oxides are less soluble than oxides of Mn, and therefore Fe is quickly trapped in sediments. Fe enrichment is more a function of times of seafloor spreading and proximity to mid-ocean ridge areas than is Mn. During spreading periods, Fe and Mn could have simultaneously precipitated if the site had been close to the ridge, but if it had been farther from the ridge, only Mn would have precipitated. For lower Miocene upward through the present sediments (at least for Biscay Bay Holes 398 and 400A), one can observe an increase in the Fe content of the sediments. This is probably the result of a detrital supply of particulate or soluble Fe or both.

The relationship of Fe concentration to the percentage of carbonates and to depth seems more complicated than that for Mn and requires more elaborate study.

CONCLUSIONS

The comparison of Sr, Mg, Fe, and Mn distributions in Holes 549 and 550B with those of the other Atlantic sites leads us to make the following conclusion.

1. The negative Sr/Mg correlation, related to carbonate diagenesis, has been confirmed for at least the Tertiary sediments. The neoformed calcites are enriched in Mg and depleted in Sr by exchange with interstitial waters.

2. It is not clear what factors play a dominant role during carbonate diagenetic transformations. It would seem that Mg diagenesis is a relatively rapid phenomenon, sensitive to the individual sedimentation rates of each time period, whereas Sr diagenesis is more likely a longer term phenomenon, sensitive to the overall sedimentation rate at the site and particularly to the residence time of sediments in a given diagenetic environment. Consequently, Sr loss from pelagic carbonates could serve as a rough method of dating individual sediment layers.

3. The data from Hole 549 show a break in Sr and Mg curves between Tertiary and Cretaceous time. This may be the result of variations in the seawater chemistry, but the influence of a change in the sedimentation rate should also be considered.

4. The results enable us to specify the influence of different factors (e.g., volcano-hydrothermal activity of the mid-ocean ridge, depth of sedimentation, $CaCO_3$ dis-

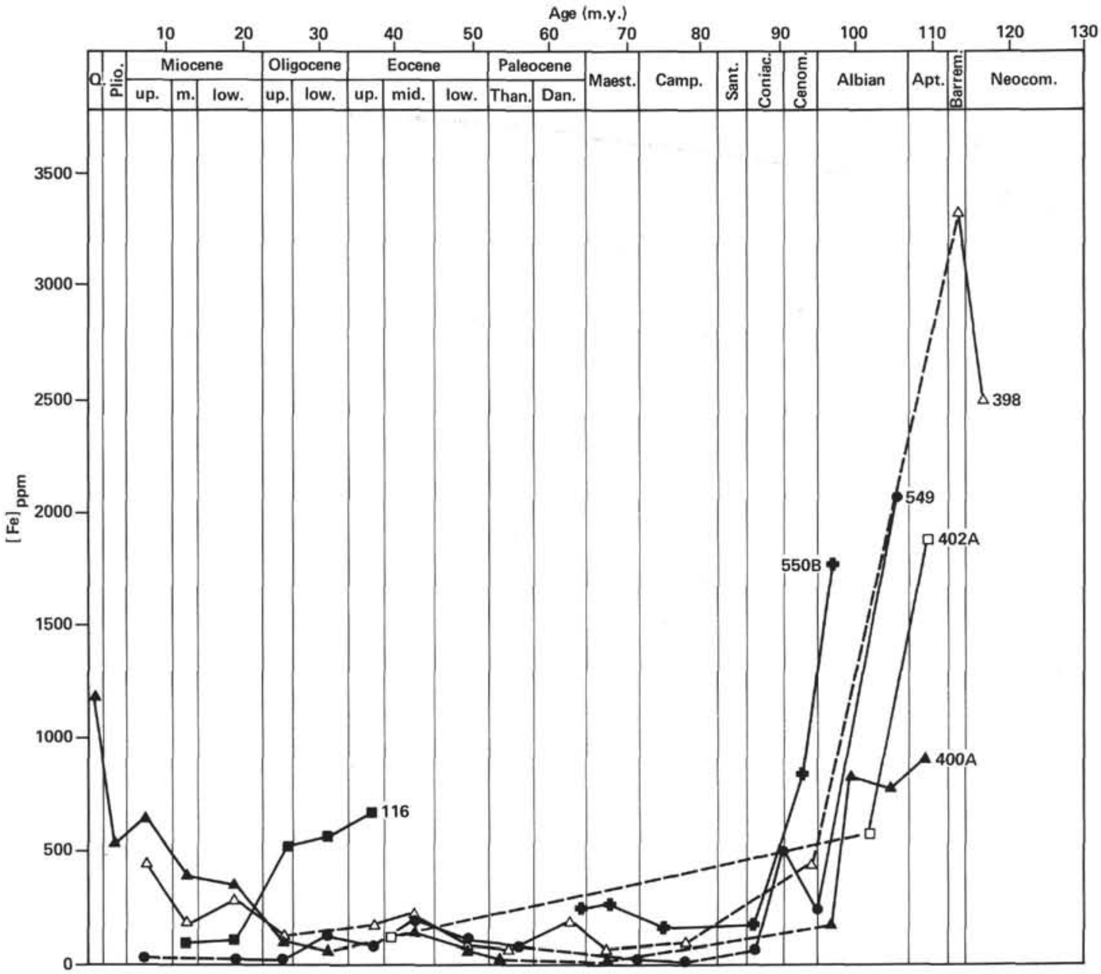

Figure 15. Average Fe contents of sediments in the North Atlantic sites. Dashed line as in Fig. 1.

solution, redox state of the medium, and distance from the ridge) on the Fe/Mn distribution in pelagic sediments and to conclude that the nature of the substratum, whether continental or oceanic, does not play an important role in the trace element content of the overlying sediments.

ACKNOWLEDGMENTS

The authors gratefully acknowledge P. C. de Graciansky for discussions and for supplying samples and J. Gieskes and J. Veizer for their helpful reviews of this paper. Thanks are extended to A. Altman and J. P. Peypouquet for their help during sampling at Lamont Doherty Geological Observatory, and to J. Gieskes for communication concerning interstitial water chemistry at Sites 540–550. Many thanks are also due to M. Gilbert Richebois and Mrs. Eva Truptil for their laboratory assistance and to Mrs. Anne Demond for typing the manuscript.

Funds for this research were provided by B.R.G.M. and by C.N.R.S. through ATP GGO.

REFERENCES

Andrianiazy, A., 1983. Influences des conditions de sédimentation et de diagenèse sur le comportement geochimique des éléments traces (Sr, Mg, Fe, Mn) des carbonates pélagiques de Sites 543 et 550 (D.S.D.P. Leg 80). Applications à l'Albien des Sites 369A, 402A, 418B, du domaine vocontien et du bassin de Paris [Thèse 3ème cycle]. Mem. 83-50, Univ. Pierre et Marie Curie, Paris.

Baker, P. A., Gieskes, J. M., and Elderfield, H., 1982. Diagenesis of carbonates in deep-sea sediments—evidence from Sr/Ca ratios and interstitial dissolved Sr^{2+} data. *J. Sediment. Petrol.*, 52:71–82.

Boström, K., and Peterson, M. N. A., 1966. Precipitates from hydrothermal exhalations on the East Pacific Rise. *Econ. Geol.*, 61: 1258–1265.

Curry, D., and Odin, G. S., 1982. Dating of the Paleogene. *In* Odin, G. S. (Ed.), *Numerical Dating in Stratigraphy:* New York (Wiley).

Doche, J. L., 1976. Les hiatus de sédimentation dans les forages du project JOIDES-DSDP. *Mem. Int., Soc. Nat. Pet. Aquitaine.*

Elderfield H., Gieskes, J. M., Baker, P. A., Oldfield, R. K., Hawkesworth, C. J., and Miller, R., 1982. $^{87}Sr/^{86}Sr$ and $^{18}O/^{16}O$ ratios, interstitial water chemistry and diagenesis in deep-sea carbonate sediments of the Ontong Java Plateau. *Geochim. Cosmochim. Acta*, 46:2259–2268.

Fischer, A. G., and Arthur, M. A., 1977. Secular variations in the pelagic realm in deep water carbonate environments. *Spec. Publ. Soc. Econ. Paleontol. Mineral.*, 25:19–50.

Gieskes, J. M., 1976. Interstitial water studies, Leg 33. *In* Schlanger, S. O., Jackson, E. D., et al., *Init. Repts. DSDP*, 33: Washington (U.S. Govt. Printing Office), 563–570.

Graham, D. W., Bender, M. L., Williams, D. F., and Keigwin, L. D., 1982. Strontium-calcium ratio in Cenozoic planktonic foraminifera. *Geochim. Cosmochim. Acta*, 46:1281–1292.

Harrison, R. K., Knox, R. W. O., Morton, A. C., Merriman, R. J., and Wheatley, C. W., 1979. Petrography and mineralogy of volcanogenic sediments from DSDP Leg 48, South-West Rockall Plateau, Sites 403 and 404, *In* Montadert, L., Roberts, D. G., et al., *Init. Repts. DSDP*, 48: Washington (U.S. Govt. Printing Office), 771–786.

Katz, A., Sass, E., Starinsky, A., and Holland, H. D., 1972. Strontium behavior in the aragonite-calcite transformation: An experimental study at 40–98°C. *Geochim. Cosmochim. Acta*, 36:481–496.
Kennedy, W. J., and Odin, G. S., 1982. The Jurassic and Cretaceous time scale in 1981. *In* Odin, G. S. (Ed.), *Numerical Dating in Stratigraphy:* New York (Wiley).
Kinsman, D. J. J., 1969. Interpretation of Sr^{2+} concentrations in carbonate minerals and rocks. *J. Sediment. Petrol.*, 39:486–508.
Klinkhammer, G. P., 1980. Observations of the distribution of manganese over the East Pacific Rise. *Chem. Geol.*, 29:211–226.
Kroopnick, P., Weiss, R. F., and Craig, H., 1972. Total CO_2, ^{13}C and dissolved oxygen—^{18}O at Geosecs II in the North Atlantic. *Earth Planet. Sci. Lett.*, 16:103–110.
LePichon, X., 1968. Sea floor spreading and continental drift. *J. Geophys. Res.*, 73:3661–3697.
Lorens, R. B., Williams, D. F., and Bender, M. L., 1977. The early nonstructural chemical diagenesis of foraminiferal calcite. *J. Sediment. Petrol.*, 47:1602–1609.
Manheim, F. T., and Sayles, F. L., 1971. Interstitial water studies on small core samples, Deep Sea Drilling Project, Leg 8. *In* Tracey, J. I., Jr., Sutton, G. H., et al., *Init. Repts. DSDP*, 8: Washington (U.S. Govt. Printing Office), 857–869.
Michard, G., 1969. Contribution à l'étude du comportemant du manganèse dans la sédimentation [Ph.D. dissert.]. Université de Paris.
Odin, G. S., Renard, M., and Vergnaud Grazzini, C., 1982. Geochemical events as a mean of correlation. *In* Odin, G. S. (Ed.), *Numerical Dating in Stratigraphy:* New York (Wiley), pp. 37–71.
Rabussier, D., 1980. Variations de composition isotopique de l'oxygène et du carbone en milieu marin et coupures stratigraphiques du Cénozoïque [Thèse 3ème cycle]. Université Pierre et Marie Curie, Paris.
Renard, M., in press. Géochimie des carbonates pélagiques: mise en évidence des fluctuations de la composition chimique des eaux océaniques depuis 140 Ma. Essai de chimiostratigraphie [Thèse d'État]. Univ. Pierre et Marie Curie, Paris.
Renard, M., and Blanc P., 1971. Mise au point d'un protocole expérimental pour le dosage d'éléments en traces (V, Cr, Mn, Ni, Sr, and Mo) par absorption atomique. *C. R. Acad. Sci.*, 272:2285–2288.
________, 1972. Influence des conditions de mise en solution (choix de l'acide, température et durée d'attaque) dans le dosage des éléments en traces des roches carbonatées. *C. R. Acad. Sci.*, 274: 632–635.
Renard, M., Delacotte, O., and Létolle, R., 1982. Le strontium et les isotopes stables dans les carbonates totaux de quelques sites de l'Atlantique et de la Téthys. *Bull. Soc. Geol. Fr.*, 7th Series, 24: 519–534.
Renard, M., Létolle, R., and Bourbon, M., 1978. Some trace elements in the carbonate samples recovered from Holes 390, 390A, 391C, and 392A of Leg 44. *In* Benson, W. E., Sheridan, R. E., et al., *Init. Repts. DSDP*, 44: Washington (U.S. Govt. Printing Office), 557–566.
Renard, M., Létolle, R., and Richebois, G., 1979. Some trace elements and their relation to oxygen and carbon isotopes in the carbonate samples recovered from Hole 400A of DSDP. Leg 48, *In* Montadert, L., Roberts, D. G., et al., *Init. Repts. DSDP*, 48: Washington (U.S. Govt. Printing Office), 727–740.
Renard, M., Richebois, G., and Létolle, R., 1979. Strontium, manganese, and iron contents, and oxygen isotopes in the carbonate fractions recovered from Hole 398C, Leg 47B. *In* Ryan, W. B. F., Sibuet, J. C, et al., *Init. Repts. DSDP*, 47, Pt. 2, Washington (U.S. Govt. Printing Office), 497–506.
________, 1983. Trace element and stable isotope geochemistry of Paleocene to Coniacian carbonate samples from Hole 516F, comparison with North Atlantic and Tethys sites. *Init. Repts. DSDP*, 72: Washington (U.S. Govt. Printing Office), 399–420.
Roberts, D. G., Montadert, L., and Searle, R. C., 1979. The western Rockall Plateau: stratigraphy and structural evolution. *In* Montadert, L., Roberts, A. G., et al., *Init. Repts. DSDP*, 48: Washington (U.S. Govt. Printing Office), 1061–1088.
Walls, R. A., Ragland, P. C., and Crisp, E. L., 1977. Experimental and natural early diagenetic mobility of Sr and Mg in biogenic carbonates. *Geochim. Cosmochim. Acta*, 41:1731–1737.
Williams, C. A., 1975. Sea-floor spreading in the Bay of Biscay and its relationship to the North Atlantic. *Earth Planet Sci. Lett.*, 24: 440–456.

Date of Initial Receipt: April 25, 1983
Date of Acceptance: November 8, 1983